EUROPEAN JOURNAL OF CANCER 42 (2006) 3253–3259

available at www.sciencedirect.com

ScienceDirect

journal homepage: www.ejconline.com

Hyaluronectin modulation of lung metastasis in nude mice

Sébastien Paris[a,*], *Richard Sesboüé*[b], *Claude Chauzy*[c], *Catherine Maingonnat*[c], *Bertrand Delpech*[c]

[a]*Animal Cell Technology Group, Biotechnology Research Institute, National Research Council Canada, 6100 Royalmount Avenue, Montreal, Quebec, Canada H4P 2R2*
[b]*INSERM U614, Rouen F-76000, France*
[c]*Laboratoire d'Oncologie Moléculaire, Centre Henri Becquerel, Rouen F-76000, France*

ARTICLE INFO

Article history:
Received 17 March 2006
Received in revised form
15 June 2006
Accepted 21 June 2006
Available online 23 August 2006

Keywords:
H460M^{GFP}
Hyaluronectin
Hyaluronic acid
Hyaluronidase
Metastasis

ABSTRACT

Hyaluronectin (HN) is a glycoprotein with a high affinity to hyaluronic acid (HA) and known to be a component of the extracellular matrix of tumours. Clinical studies have shown that a low level of HN correlates to tumours with poor prognosis, whereas a high level of HN correlates to tumours with good prognosis. We previously demonstrated *in vitro* that hyaluronidase activity, which promotes tumour progression and metastatic spread by degradation of HA into angiogenic oligosaccharides, was inhibited or promoted by HN, according to the level of HN-expression. This raises the question of the role played by HN in cancer, and particularly if high and low levels of HN-expression could trigger opposite effects on tumour growth and/or metastatic spread. To address this issue, we used a model of spontaneous lung fluorescent metastases that we characterised previously. We stably transfected the human HN cDNA into fluorescent H460M^{GFP} cells and selected two clones characterised by different levels of HN-expression: HN110 and HN704, with a high and a low level of HN-expression, respectively. *In vitro*, we demonstrated that HN704 cell migration was significantly increased. Inoculation of clones to nude mice had no significant effect on tumour growth, but clearly revealed opposite effects on metastatic spread: HN110 significantly decreased the number of fluorescent metastases whereas HN704 significantly increased it. We also analysed HN, HA and hyaluronidase contents in sera and tumours. These results demonstrate that HN can play a role as either a suppressor or promoter of metastatic spread.

1. Introduction

During tumour development, cancerous cells induce numerous changes in their microenvironment. The modifications of the extracellular matrix trigger a set of physiological responses such as development of new blood vessels (neo-angiogenesis), allowing tumour growth to carry on, or migration of cancerous cells towards blood vessels, leading to spread of metastases. Hyaluronic acid (HA), also known as hyaluronan, is a major component of the extracellular matrix, which is greatly implicated in several of these responses.[1] The degradation of this polysaccharide into small angiogenic fragments by hyaluronidases promotes tumour growth[2] and metastatic spread by triggering endothelial cell migration and capillary formation.[3–5] Hyaluronectin (HN), a glycoprotein discovered in 1979 in brain and in cancer tumour stroma,[6] exhibits a great affinity for HA.[7] The amino acid sequence of HN matches perfectly with that of the HA-binding domain of

* *Corresponding author:* Tel.: +1 514 496 7391; fax: +1 514 496 6785.
E-mail address: sebastien.paris@cnrc-nrc.gc.ca (S. Paris).
0959-8049/$ - see front matter
doi:10.1016/j.ejca.2006.06.012

versican, a large proteoglycan.[8] HN/HA complexes dissociate at acidic pH, which allow purification of HN by affinity chromatography on insolubilised HA.[9,10] Studies made with antibodies directed against the HA-binding domain of versican located the versican HA-binding domain to the nodes of Ranvier,[11] a well-known location of HN.[12,13] The association of HN with cancer stroma led to the question of whether this protein could play a role in cancer development, likely as a modulator of HA. Indeed, in brain tumours, the HN/HA ratio is much lower in glioblastomas than in low-grade astrocytomas.[14] In breast cancer, we find that medullary tumours, whose prognosis is better than that of other breast adenocarcinomas, were characterised by HN-rich mononuclear infiltrates.[15] HN release by monocytes is modulated by interleukins.[16] *In vitro*, HN inhibits the promotion of endothelial cell migration by HA-derived oligosaccharides,[17] suggesting that HN can exert an anti-angiogenic effect *in vivo*. Moreover, HN is also able to inhibit *in vitro* hyaluronidase activity of cancer cells at pH 3.8 at concentrations above 100 μg/ml, whereas this activity is very efficiently enhanced at concentrations below 50 μg/ml.[18,19]

In the present work, we evaluated *in vivo* the impact of different levels of HN-expression on tumour growth and metastatic spread. We took advantage of a model of fluorescent spontaneous lung metastases that we developed in nude mice[20,21] to demonstrate that, according to the level of expression, HN could act as either a promoter or suppressor of metastatic spread. These results provide the first evidence for the implication of HN as a modulator of metastatic spread, and suggest a complex mode of action.

2. Materials and methods

2.1. Cell lines and culture

The H460M^{GFP} cell line was obtained and characterised as previously described.[20,21] This cell line was derived from the H460M cell line and stably expresses the cDNA of the Green Fluorescent Protein (GFP). All cell lines were maintained as adherent monolayers in RPMI-1640 medium (Life Technologies, Pontoise, France) supplemented with 10% foetal calf serum (Roche Diagnostic, Meylan, France) and 2 mM L-glutamine (Life Technologies, Pontoise, France) at 37 °C in a humidified incubator with 5% CO_2 in air. The cells were grown to 80% confluence, washed two times with phosphate buffered saline and then harvested after a brief treatment with trypsin/EDTA (Sigma, Saint-Quentin Fallavier, France). Cell viability was determined by trypan blue dye exclusion.

2.2. Construction of a recombinant expression vector containing the human HN cDNA

The pBlueScript vector (Stratagene) containing the cDNA of the HA-binding domain of versican[8] was kindly provided by Dr. Zimmerman (Department of Pathology, University of Zurich, Switzerland). This cDNA was inserted into the bicistronic mammalian expression vector pIRES-Hyg (Clontech, Palo Alto, USA), allowing the selection of mammalian cells by expression of hygromycin B resistance. The inserted sequence, cloned into *Bam*HI and *Bst*XI restriction sites of pIRES-Hyg vector, extends from nucleotides 1–1372 of the human versican N-terminus portion and corresponds to the whole human HN sequence. The final vector, used for transfections and encoding the human HN protein, was named pHN-IRES-Hyg.

2.3. Transfection and isolation of cellular clones expressing HN

The H460M^{GFP} cell line was used as the parental cell line to obtain HN-expressing cells. Transfections were performed in near confluent cells by the Fugene-6 procedure (Roche, Meylan, France). One day before transfection, cells were seeded at a density of 3×10^5 cells in 35-mm culture dishes (Corning Costar, Brumath, France). For transfection, 6 μl of Fugene-6 reagent were diluted in 94 μl of serum-free medium. The solution was incubated for 10 min with 2 μg of vector and then added to the cells. The cells were harvested by trypsin/EDTA for 24 h after transfection, and subcultured at a ratio of 1:10 in a selective medium that contained 200 μg/ml of Hygromycin B (Clontech). Ten to 14 days after selection, surviving cells were cloned by limiting dilution. Individual clones were expanded and screened for HN-expression.

2.4. Microscopy and cytofluorimetry

Microscopic evaluation of GFP-expression in cell lines was performed as previously described[20,21] by direct observation of cells using a fluorescence microscope (Axiovert 10, Zeiss) equipped with a double-pass filter set for FITC/PI (excitation filter BP450-490; suppression filter LP520). Cell lines fluorescence was analyzed by FACS (FACS Calibur, Becton Dickinson, Omaha, CA) with a standard excitation wavelength of 488 nm.

2.5. HN determination

HN was quantitated by ELISA using HA-coated (to test the affinity to HA) and antibody-coated plastic microplates as previously described;[9] both techniques gave similar results ($R^2 = 0.96$). The use of antibody-coated plates allowed digestion of the samples with bovine testicular hyaluronidase before the assay to establish that no HN would be masked by HA. Briefly, samples were diluted in 10 mM sodium phosphate buffer containing 1 M NaCl, 0.2 g/l EDTA, 0.25 g/l sodium azide and 1 g/l BSA, at pH 7.4 and incubated in plate wells for 3 h at 4 °C. HN bound to the plate was measured with alkaline phosphatase-linked rabbit antibodies to human HN, and staining was performed with *p*-nitrophenyl phosphate at pH 9.8.

2.6. Western blot analysis

HN detection was performed on concentrated serum-free culture medium. HN was precipitated from the culture medium by addition of saturated ammonium sulfate at 4 °C for 48 h. The precipitate was dissolved in PBS (1/10 of the initial volume), dialyzed against PBS and HN content was determined with the ELISA method. Twenty microlitre samples were electrophoresed in 0.2% SDS w/v on 15% polyacrylamide v/v gel with a 4% v/v stacking gel according to Laemmli[22] for 40 min (Hoeffer, Bioblock, Strasbourg, France). Electrophoretic

transfer to nitrocellulose sheets (BA 83 from Schleicher and Schuell, Céra Labo, Aubervilliers, France) was performed in a horizontal device (Biolyon, Lyon, France) under 20 V for 1 h. After saturation with 10 g/l bovine serum albumin (Sigma) in PBS for 1 h at 37 °C, sheets were incubated for 1 h at 37 °C with rabbit anti-human brain HN antibodies (0.5–1 mg/l) in PBS containing 10 g/l bovine serum albumin and 1 g/l Tween 20. When monoclonal antibodies were used, they were detected with the ABC kit from Vectastain (Biosys, Compiègne, France). Washings were performed in PBS with 1 g/l Tween 20, 3 × 5 min, at room temperature. Alkaline phosphatase-conjugated donkey antibodies to rabbit IgG were incubated 1/5000 to 1/10,000 for 30 min at 37 °C in PBS-Tween-albumin buffer. After three 5 min washings, sheets were stained with the *p*-nitro-blue-tetrazolium chloride/bromo-chloro-indolyl-phosphate procedure.[23] In order to study HN glycosylation, 20 μl of concentrated culture medium was supplemented with 0.5 μl of 500 mM phenanthroline in methanol and incubated for 18 h at 37 °C with 0.5 μl of recombinant *N*-glycanase (Genzyme, Cergy Pontoise, France) at 250 U/ml and analyzed by Western blotting. A control was made replacing *N*-glycanase by 0.5 μl water.

2.7. Cell doubling time

Cells were seeded at 6×10^4 in 60-mm culture dishes. At daily intervals, triplicate samples were harvested by trypsinisation. A 100 μl aliquot of cell suspension was added to 100 μl of trypan blue (Sigma) and counted using a Malassez cell. The doubling time was calculated from the cell growth curve over 5 days.

2.8. Cell migration assay

Chemotaxis of tumour cells was determined using Transwell cell culture chamber inserts (Corning Costar, Brumath, France) with a 24-mm diameter polycarbonate filter with 8-μm pore size. The conditioned medium, used as chemoattractant, was obtained from a H460M cell culture as previously described.[20] Five hundred microlitres of a cell suspension at 10^6 cells/ml of serum-free medium was added to the upper compartment and the lower compartment was filled with 1.8 ml of conditioned medium. After 24 h at 37 °C, the medium of the upper surface of the filter was removed and the Transwell was treated with acetic-alcohol fixative for 10 min, then washed. Cells of the upper compartment were removed by scraping with a cotton tip. The number of migrating cells was determined after Crystal violet staining, as previously described.[21]

2.9. Primary tumours and spontaneous fluorescent lung metastases in nude mice

Animal experiments were performed in accordance to the regulations of the institutional ethical commission. Specific-pathogen-free female Swiss homozygous *nu/nu* mice, 6–8 weeks old, were obtained from Iffa Credo (L'Arbresle, France) and maintained under barrier conditions throughout the study. For *in vivo* studies, 16 animals per cell line were injected subcutaneously in flanks with 5×10^6 cells in 200 μl of RPMI-1640 medium. $H460M^{GFP}$ cells transfected by pIRES-Hyg vector were used as control (Mock). Mice were sacrificed 28 days later by ether inhalation. Blood was taken from the eye vein for HN, HA and hyaluronidase assays. Primary tumours were excised and weighed. Tumour extracts for HN, HA and hyaluronidase assays were prepared by grinding tumour (1 g) on ice in 4 ml distilled water supplemented with protease inhibitors (Sigma, Saint-Quentin Fallavier, France). Fluorescent lung metastases were studied as previously described;[20,21] briefly, each whole lung lobe was placed and tightly held between two glass slides. The same methodology was used for intestine, heart and liver sliced in thin sections. GFP-expressing metastases were counted under fluorescence microscopy.

2.10. HA determination in tumours

The tumour HN was quantitated via ELISA technique on HA-coated plates as described.[6] Briefly, the samples were digested with protease (l mg/ml) overnight at 37 °C. Protease was inactivated at 100 °C for 10 min and the samples were centrifuged at 13,000*g* for 10 min. Dilutions of the samples were supplemented with alkaline phosphatase-linked HN and incubated at 4 °C for 4 h on HA-coated plate. Staining of alkaline phosphatase bound to plate HA was made with *p*-nitrophenyl phosphate at pH 9.8.

2.11. Hyaluronidase assays

Hyaluronidase was measured in all cases at pH 3.8 by reference to human serum whose hyaluronidase content was determined using the Reissig technique. The digestion of HA bound to plastic microtest plates was measured with alkaline phosphatase linked HN, as previously described.[6]

2.12. Statistical analysis

All statistical analyses were performed using the non-parametric Mann–Whitney test. Differences between control and experimental groups were considered statistically significant at $p < 0.05$.

3. Results

3.1. Isolation and characterisation of stable transfectants

Transfections were performed to obtain stable fluorescent clones expressing different levels of HN. To address this issue, $H460M^{GFP}$ cells were stably transfected by pHN-IRES-Hyg and cultured in selective medium as described in Section 2. $H460M^{GFP}$ cells were also stably transfected by the pIRES-Hyg vector and a clone was used as control (mock). HN-transfected clones were characterised with respect to HN and GFP-expression (only GFP for mock cells). This led to the selection of two HN-expressing stable clones, HN110 and HN704, which were chosen for their different HN-expression levels (Table 1). These measures correspond to a *de novo* expression of HN, as HN could not be detected in mock cells.

HN was characterised by its affinity for HA as shown by the ELISA test. Its molecular size measured on blots (Fig. 1) was in good agreement with the expected size (45 kDa). Fig. 1 (lanes

Table 1 – HN cellular synthesis in culture medium and in vitro analysis of cell migration

Cell line	HN synthesis (fg/cell/h)	Cell migration (%)
Mock	0	100 ± 10
HN110	11	80.6 ± 12.5
HN704	3	158.9 ± 5.2*

The results were analyzed using the non-parametric Mann–Whitney test against mock used as control of three independents experiments. Difference from mock: $^{*}p < 0.05$.

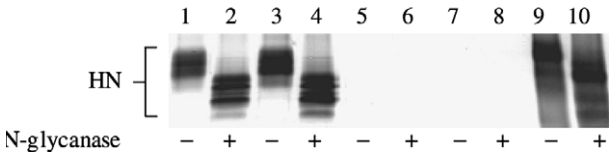

Fig. 1 – Western blot analysis of HN-expression in transfected cells. Concentrated serum-free medium was digested (+) or not digested (–) by N-glycanase before gel electrophoresis. Lanes 1–2, HN110, lanes 3–4, HN704, lanes 5–6, H460M^{GFP} transfected by pIRES-Hyg vector (mock), lanes 7–8, H460M cells, lanes 9–10, human cerebral HN. Two hundred nanograms was loaded for each sample, except for HN704 (340 ng) and human brain HN (1 μg). The profile obtained indicates that post-transductional modifications occur correctly on the recombinant HN before its secretion in culture medium. This expression profile could be observed after two months in culture without hygromycin B.

5–8) confirms the absence of HN-expression in controls. After N-glycanase digestion of culture extracts, HN showed several smaller forms corresponding to different glycosylated HN molecules, with patterns similar to those observed with HN purified from normal human brain. In the absence of hygromycin B, HN-expression of both clones remained stable for up to 2 months while in exponential growth conditions (data not shown).

Fluorescence of clones could easily be monitored by fluorescent microscopy (data not shown) or cytofluorimetry of living cells. GFP-expression remained stable up to 2 months in transfected H460M^{GFP} cells in exponential growth culture conditions without geneticin, with fluorescence profiles and intensities of HN-transfected clones similar to those of corresponding control (data not shown). No difference was observed in cell morphology (data not shown).

3.2. *In vitro analysis: doubling time and chemotaxis*

Comparison of cell proliferation rates between mock and HN-transfected cell lines was identical, with a calculated *in vitro* doubling time of 18–24 h for all cell lines. Analysis of cell chemotaxis showed that HN704 cells dramatically increased their capacity to migrate through a Transwell membrane. This led to almost 60% more migrating cells for HN704 than mock cells (Table 1). In contrast, we observed a slight decrease of about for 20% of HN110 cells chemotaxis when compared to mock cells.

3.3. *Tumour growth and metastasis formation*

To determine the impact on tumour growth and metastasis spread of HN-expression in mice grafted with mock, HN110, or HN704 clones, 16 nude mice were inoculated as described in Section 2. Twenty-eight days post-inoculation, mice were sacrificed, tumours were excised and lungs were analyzed under fluorescent microscopy as previously described.[20] The variations of primary tumour weights observed for both HN-expressing clones were not significantly different from those of mock (Fig. 2(a)) with medians comprised between 1.24 and 1.45 g. Nevertheless, we could observe that the upper quartile for HN704 (2.91 g) is greater than the upper quartiles for mock and HN110 with values of 2.1 g and 2.16 g, respectively (Fig. 2(a)).

A significant decrease of the fluorescent lung metastases number was observed with HN110 cells with respect to control: the interquartile ranges were 1–16 versus 7–54 ($p = 0.013$) for HN110 and mock, respectively (Fig. 2(b)). Conversely, a significant increase of the fluorescent lung metastases number was observed with HN704 cells (interquartile ranges: 46–95) with respect to mock ($p = 0.003$) (Fig. 2(b)). As previously reported,[21,24] no metastasis could be detected in other analysed tissues (liver, intestine and heart), in mock, HN110 and HN704 grafted mice.

Scatter plots (Fig. 3) showed that the decrease observed in the number of metastases for HN110 was not related to a reduction of tumour weight. Also, the increase in the number of metastases observed for HN704 was not related to an increase in tumour weight.

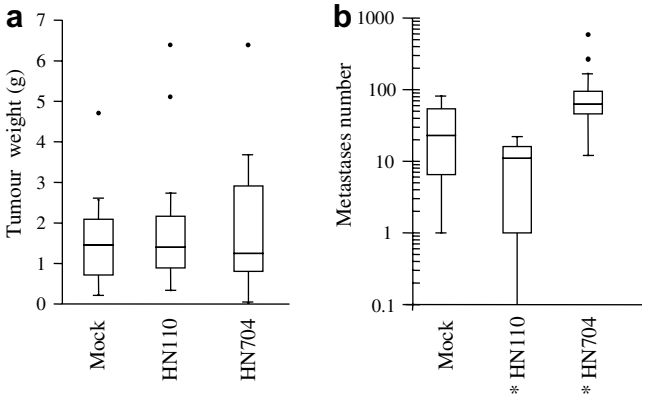

Fig. 2 – Box and whisker plots of primary tumour weights (a) and number of fluorescent lung metastases (b). Mice grafted with mock, HN110 or HN704 cells were sacrificed four weeks after s.c. injection. The primary tumours were excised and weighted. Each whole lung lobe was placed between two glass slides and the number of metastases was determined under fluorescent microscopy. Sixteen mice were analysed for both mock and HN-expressing clones. The results were analysed using the non-parametric Mann–Whitney test. Difference from control: $^{*}p < 0.05$.

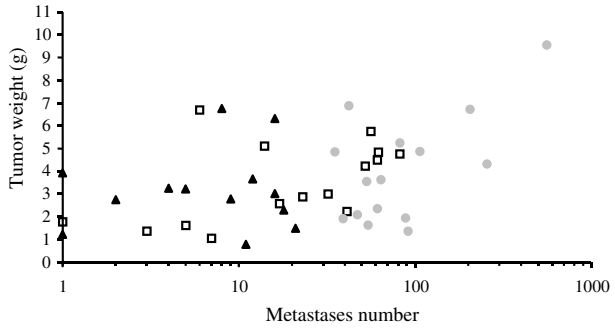

Fig. 3 – Scatter plots of primary tumour weight versus metastases number: mock (□), HN110 (▲), HN704 (●). The number of fluorescent lung metastases could not be related to the weight of the tumour.

3.4. *HN, HA and hyaluronidase expression in mouse sera*

To determine HN, HA and hyaluronidase-expression, the sera of grafted mice were taken 28 days after s.c. injections of HN-expressing cells and mock cells. HN concentration in the sera of mice grafted with HN-clones was significantly increased with respect to the serum concentration of mice grafted with mock cells (Fig. 4). HN level in the sera of HN110 grafted mice is almost 7-fold greater than the sera of HN704 grafted mice, and 50-fold than the sera of mock grafted mice. No significant difference could be found between serum HA concentrations and hyaluronidase activities for both HN-expressing clones and mock (data not shown).

3.5. *HN, HA and hyaluronidase expression in tumour extracts*

HN, HA and hyaluronidase-expression were analysed in excised tumours. HN was significantly increased in tumour extracts derived from both HN-expressing clones (~71-fold for HN110 and ~14-fold for HN704), by comparison with the content of the tumours obtained with the mock (Fig. 4). Moreover, HN level in tumours induced by HN110 cells is ~5-fold greater than in tumours induced by HN704 cells. HA was increased in tumours extracts for both HN-expressing clones, when compared to the content of the tumours obtained with the mock (Table 2). An increase greater than 2-fold could be observed for HA in tumour extracts from HN110 grafted mice, but only about 1.5-fold in tumour extracts from HN704 grafted mice. No significant difference between hyaluronidase expression from tumours extracts from HN-expressing clones and mock could be observed (data not shown).

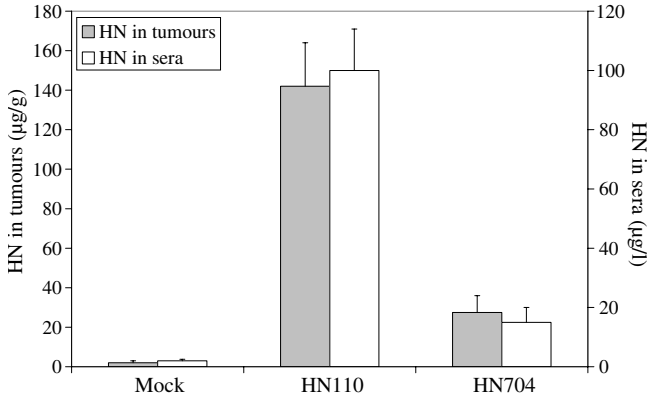

Fig. 4 – HN contents in sera and tumours in mice grafted with mock, HN110, or HN704 cells. Blood samples of sacrificed mice were collected, and HN was determined using ELISA method on HA-coated (to test the affinity to HA) and antibody-coated plastic microplates. Mean ± SD, *n* = 16.

Table 2 – In vivo analyze of HA contents in tumours

Cell line	HA (mg/g)
Mock	13 ± 4
HN110	27 ± 7*
HN704	19 ± 8

The results were analyzed using the non-parametric Mann–Whitney test against mock used as control. Mean ± standard deviation. *n* = 16. Difference from mock: $^{*}p < 0.05$.

4. Discussion

In the present study, we used an *in vivo* sensitive cellular assay[20,21,24] to determine the effect of HN-expression on tumour growth and metastatic spread. The cell line H460M^{GFP} used in this work induces numerous lung metastases when injected to nude mice. The stable expression of the GFP by these cells allows us to visualise H460M^{GFP} cells up to unicellular level directly in fresh host tissues by fluorescent microscopy and allowing us to determine the total number of metastases. Using this model, we provide evidence that different levels of HN-expression could modulate the metastases by two opposing ways.

We obtained two stable GFP and HN-expressing clones by transfection of the human cDNA in the non-secreting HN H460M^{GFP} cell line. In both cases, the transfection resulted in secretion into the culture medium of glycosylated forms of HN similar to those extracted from brain and tumours and also found in the culture medium of monocytes and fibroblasts.[10] This indicated that post-transductional modifications of the recombinant HN protein were correctly performed by the cell before its secretion into the culture medium.

In vitro, we demonstrate that HN704 cells chemotaxis was dramatically increased when compared to mock and HN110 cells. This result suggested that the low HN-expression level of HN704 cells (3 fg/cell/h) could enhance cell migration, a feature that has not been previously reported for HN. The biological pathways leading to this enhanced cell migration capacity remain to be elucidated. On the other hand, we demonstrated that HN110 cells chemotaxis is decreased, which is in good agreement with that previously reported for endothelial cell migration *in vitro*.[17] HN-expressing clones have a doubling time similar to that of mock in culture, thus indicating that HN-expression did not interfere with cell growth.

As the GFP and HN-expression levels of these clones remain stable in culture without hygromycin B or geneticin

for at least two months, we considered that these clones were suitable for *in vivo* experiments. Therefore, mice were sacrificed 28 days after cell inoculations. Independent of the clone studied, the cells displayed a remarkably stable fluorescent signal, allowing easy tracking of metastases in host tissues.[20,21,24] The sera of grafted mice and the stroma of the tumours obtained with both HN-expressing clones contained human HN, as characterised by its antigenic features and affinity for HA. Conversely, the control sera and tumours did not contain any significant amounts of human HN. The HN contents observed for HN110 and HN704 cells demonstrated overall consistent parallels between culture medium, tumour extracts and sera levels in grafted mice.

No significant variation of tumour growth could be observed between HN-expressing clones and the control. This result indicated that the neo-angiogenesis remains sufficient to provide oxygen and nutrients to the tumours in all cases, and also suggested that HN did not have anti- nor pro-angiogenic effects *in vivo* as we would expect for HN110- and HN704-grafted mice, respectively. Indeed, the results obtained with the HN110 grafted mice are in contradiction with not only the inhibitory effects of HN on the promotion of endothelial cell migration previously reported,[17] but also with its capacity to inhibit hyaluronidase, both events expected at least to limit the neo-angiogenesis activity. This apparently contradictory result could be explained by previous studies[25,26] documenting that H460 cells produce FGF2 and VEGF, two factors well known to induce neo-angiogenesis. We postulate that these factors are sufficiently strong to induce neo-angiogenesis and to hide the inhibitory effect of HN on neo-angiogenesis. Moreover, the results obtained for tumour growth with HN704 seem also in contradiction with previous studies showing that low level of HN-expression can efficiently enhance hyaluronidase activity, triggering HA degradation and generating angiogenic fragments, thus leading to an increase of tumour growth due to better neo-angiogenesis. Nevertheless, the increase of tumour growth observed for the upper quartile of HN704 grafted mice suggested that tumour growth could be effectively enhanced. This result is probably not related to a better cell growth, as the cell doubling time *in vitro* is similar for all cell lines. We postulate that a more significant increase of tumour growth would be detected if mice had been sacrificed at 7 or 8 weeks post-inoculation, but, as previously reported,[20] the accurate determination of the number of fluorescent lung metastases would be impaired due to fusion of metastases.

We previously reported that $H460M^{GFP}$ cells induce only lung metastases.[20,21] No change in the localisation of metastases could be observed in mock, HN110 and HN704 grafted mice, suggesting that HN does not modify homing of cancerous cells. Nevertheless, we documented that lung metastasis formation was significantly altered, in opposite ways, in comparison with the control cell line. Although significantly decreased in HN110, the number of metastases dramatically increased with HN704. The modulation of metastases spread could be in part explained by the variations of cell chemotaxis observed *in vitro*. It is well established that cancerous cells must acquire the capacity to migrate towards blood vessels before entering the blood stream and forming metastases. Therefore, enhanced cell migration capacity could result in an increase of cell spread and metastases number, as observed for HN704, whereas decrease of chemotaxis capacity would limit cell spread, preventing metastases formation, as observed for HN110.

Interestingly, the levels of HA were dramatically increased in tumour extracts from both HN-expressing clones when compared to mock tumour extracts, particularly in HN110 induced tumours. We previously reported that H460M cells do not synthesise HA,[27] indicating that HA present in tumours is produced by tumour-associated stroma. These results are in good agreement with the high affinity of HN for HA, and suggest that HN/HA association can prevent HA degradation, presumably by hyaluronidase. Furthermore, this supports the concept of inhibition of hyaluronidase activity by HN. Hyaluronidase activities are similar in both sera and tumour extracts of HN110, HN704 and mock grafted mice, indicating that hyaluronidase synthesis is not modified by HN-expression.

Thus, low production of HN in tumours could be a factor for poor prognosis, a feature that we observed in glioblastoma, whereas high HN production can have a protective effect, as observed in low-grade astrocytomas.[14] Taken together, these results demonstrate that HN acts in cancer progression as both promoter and suppressor of metastasis spread, depending on the concentration; however, the mechanism leading to these results remains to be elucidated. These results are similar to the study published recently by Lokeshwar and colleagues[28] on hyaluronidase expression in cancer cells, suggesting that the phenomenon of either promotion or suppression of cancer by HA-related molecules is more widespread than the formerly known, and further documents the importance of the role of extracellular matrix in cancer biology. Moreover, these results are in agreement with what is known of hyaluronidase activity and support the role played by hyaluronidase in metastasis formation. This study may also provide a basis for possible high HN treatments for controlling metastases and suggests that HN could be used as an indicator of prognosis of tumours. The data presented in this study are based on only one clone of each category. Due to technical difficulties, we could not obtain more than one clone, which showed exactly the same phenomenon. Thus, we cannot rule out the possibility that the observed cellular effects could also be simply the effect of the site insertion of HN cDNA in the genome. In order for these results to be confirmed, more than one clone will have to be studied. Furthermore, analysis of more than one clone will allow in the future to determine a threshold beyond which HN inhibits lung metastases.

Conflict of interest statement

None declared.

Acknowledgements

This work was supported by ARC (Association pour la Recherche sur le Cancer) and Délégation à la Recherche Hospitalière du CHU de Rouen. We thank Dr. Zimmerman for the generous

gift of versican clone F. We thank Brian Cass for his helpful assistance in writing the manuscript.

REFERENCES

1. Toole BP. Hyaluronan: from extracellular glue to pericellular cue. *Nat Rev Cancer* 2004;**4**:528–39.
2. Lokeshwar VB, Cerwinka WH, Lokeshwar BL. HYAL1 hyaluronidase: a molecular determinant of bladder tumor growth and invasion. *Cancer Res* 2005;**65**:2243–50.
3. West DC, Hampson IN, Arnold F, et al. Angiogenesis induced by degradation products of hyaluronic acid. *Science* 1985;**228**:1324–6.
4. Lees VC, Fan TP, West DC. Angiogenesis in a delayed revascularization model is accelerated by angiogenic oligosaccharides of hyaluronan. *Lab Invest* 1995;**73**:259–66.
5. Liu D, Pearlman E, Diaconu E, et al. Expression of hyaluronidase by tumor cells induces angiogenesis in vivo. *Proc Natl Acad Sci USA* 1996;**93**:7832–7.
6. Delpech B, Delpech A, Girard N, et al. An antigen associated with mesenchyme in human tumours that cross-reacts with brain glycoprotein. *Br J Cancer* 1979;**40**:123–33.
7. Delpech B. Immunochemical characterization of the hyaluronic acid–hyaluronectin interaction. *J Neurochem* 1982;**38**:978–84.
8. Zimmermann DR, Ruoslahti E. Multiple domains of the large fibroblast proteoglycan, versican. *EMBO J* 1989;**8**:2975–81.
9. Delpech B, Bertrand P, Maingonnat C. Immunoenzymoassay of the hyaluronic acid–hyaluronectin interaction: application to the detection of hyaluronic acid in serum of normal subjects and cancer patients. *Anal Biochem* 1985;**149**:555–65.
10. Delpech B, Bertrand P, Maingonnat C, et al. Enzyme-linked hyaluronectin: a unique reagent for hyaluronan assay and tissue location and for hyaluronidase activity detection. *Anal Biochem* 1995;**229**:35–41.
11. Lebaron RG. Versican. *Perspect Dev Neurobiol* 1996;**3**:261–71.
12. Delpech A, Delpech B, Girard N. Association de la glycoprotéine cérébrale (ANS 3) à la membrane du neurone et aux étranglements de Ranvier. *C R Seances Acad Sci D* 1979;**288**:1323–6.
13. Delpech B, Maingonnat C, Delpech A, et al. Characterization of a hyaluronic acid-binding protein from sheep brain comparison with human brain hyaluronectin. *Int J Biochem* 1991;**23**:329–37.
14. Delpech B, Maingonnat C, Girard N, et al. Hyaluronan and hyaluronectin in the extracellular matrix of human brain tumour stroma. *Eur J Cancer A* 1993;**29**:1012–7.
15. Delpech B, Girard N, Olivier A, et al. The origin of hyaluronectin in human tumors. *Int J Cancer* 1997;**72**:942–8.
16. Girard N, Maingonnat C, Bertrand P, et al. Hyaluronectin secretion by monocytes: downregulation by IL-4 and IL-13, upregulation by IL-10. *Cytokine* 1999;**11**:579–84.
17. Trochon V, Mabilat-Pragnon C, Bertrand P, et al. Hyaluronectin blocks the stimulatory effect of hyaluronan-derived fragments on endothelial cells during angiogenesis in vitro. *FEBS Lett* 1997;**418**:6–10.
18. Maingonnat C, Victor R, Bertrand P, et al. Activation and inhibition of human cancer cell hyaluronidase by proteins. *Anal Biochem* 1999;**268**:30–4.
19. Maingonnat C, Courel MN, Bertrand P, et al. Hyaluronidase in sera of tumour-bearing nude mice. *Biomarkers* 2003;**8**:333–8.
20. Paris S, Chauzy C, Martin-Vandelet N, et al. A model of spontaneous lung metastases visualised in fresh host tissue by green fluorescent protein expression. *Clin Exp Metastasis* 1999;**17**:817–22.
21. Paris S, Sesboue R, Delpech B, et al. Inhibition of tumor growth and metastatic spreading by overexpression of inter-alpha-trypsin inhibitor family chains. *Int J Cancer* 2002;**97**:615–20.
22. Laemmli UK. Cleavage of structural proteins during the assembly of the head of bacteriophage T4. *Nature* 1970;**227**:680–5.
23. Bestagno M, Cerino A, Riva S, et al. Improvements of Western blotting to detect monoclonal antibodies. *Biochem Biophys Res Commun* 1987;**146**:1509–14.
24. Paris S, Sesboue R. Metastasis models: the green fluorescent revolution? *Carcinogenesis* 2004;**25**:2285–92.
25. Takayama K, Ueno H, Nakanishi Y, et al. Suppression of tumor angiogenesis and growth by gene transfer of a soluble form of vascular endothelial growth factor receptor into a remote organ. *Cancer Res* 2000;**60**:2169–77.
26. Scharovsky OG, Binda MM, Rozados VR, et al. Angiogenic and antiangiogenic balance regulates concomitant antitumoral resistance. *Clin Exp Metastasis* 2004;**21**:177–83.
27. Delpech B, Courel MN, Maingonnat C, et al. Hyaluronan digestion and synthesis in an experimental model of metastatic tumour. *Histochem J* 2001;**33**:553–8.
28. Lokeshwar VB, Cerwinka WH, Isoyama T, et al. HYAL1 hyaluronidase in prostate cancer: a tumor promoter and suppressor. *Cancer Res* 2005;**65**:7782–9.